

# $\bar{B} \rightarrow X_s \gamma$ constraints on the top quark anomalous $t \rightarrow c \gamma$ coupling

Xingbo Yuan,<sup>1</sup> Yang Hao,<sup>1</sup> and Ya-Dong Yang<sup>1,2</sup>

<sup>1</sup>*Institute of Particle Physics, Huazhong Normal University, Wuhan, Hubei 430079, People's Republic of China*

<sup>2</sup>*Key Laboratory of Quark and Lepton Physics, Ministry of Education, Huazhong Normal University, Wuhan, Hubei, 430079, People's Republic of China*

(Received 18 October 2010; published 21 January 2011)

Observation of the top quark flavor changing neutral process  $t \rightarrow c + \gamma$  at the LHC would be the signal of physics beyond the standard model. If anomalous  $t \rightarrow c \gamma$  coupling exists, it will affect the precisely measured  $\mathcal{B}(\bar{B} \rightarrow X_s \gamma)$ . In this paper, we study the effects of a dimension 5 anomalous  $tc\gamma$  operator in  $\bar{B} \rightarrow X_s \gamma$  decay to derive constraints on its possible strength. It is found that, for real anomalous  $t \rightarrow c \gamma$  coupling  $\kappa_{icR}^\gamma$ , the constraints correspond to the upper bounds  $\mathcal{B}(t \rightarrow c + \gamma) < 6.54 \times 10^{-5}$  (for  $\kappa_{icR}^\gamma > 0$ ) and  $\mathcal{B}(t \rightarrow c + \gamma) < 8.52 \times 10^{-5}$  (for  $\kappa_{icR}^\gamma < 0$ ), respectively, which are about the same order as the  $5\sigma$  discovery potential of ATLAS ( $9.4 \times 10^{-5}$ ) and slightly lower than that of CMS ( $4.1 \times 10^{-4}$ ) with  $10 \text{ fb}^{-1}$  integrated luminosity operating at  $\sqrt{s} = 14 \text{ TeV}$ .

DOI: 10.1103/PhysRevD.83.013004

PACS numbers: 12.15.Lk, 13.20.He, 14.65.Ha

## I. INTRODUCTION

In the standard model (SM), a top quark lifetime is dominated by the  $t \rightarrow bW^+$  process, and its flavor changing neutral current (FCNC) processes  $t \rightarrow qV$  ( $q = u, c$ ;  $V = \gamma, Z, g$ ) are extremely suppressed by the Glashow-Iliopoulos-Maiani mechanism. It is known that the SM predicts a very tiny top FCNC branching ratio  $\mathcal{B}(t \rightarrow qV)$ , less than  $\mathcal{O}(10^{-10})$  [1], which would be inaccessible at the CERN Large Hadron Collider (LHC). In the literature [2,3], however, a number of interesting questions have been intrigued by the large top quark mass which is close to the scale of electroweak symmetry breaking. For example, one may raise the question whether new physics (NP) beyond the SM could manifest itself in nonstandard couplings of the top quark which would show up as anomalies in the top quark productions and decays.

At present, the direct constraints on  $\mathcal{B}(t \rightarrow qV)$  are still very weak. For its radiative decay, the available experimental bounds are  $\mathcal{B}(t \rightarrow u\gamma) < 0.75\%$  from ZEUS [4] and  $\mathcal{B}(t \rightarrow q\gamma) < 3.2\%$  from CDF [5] at 95% C.L., respectively. These constraints will be improved greatly by the large top quark sample to be available at the LHC, which is expected to produce  $8 \times 10^6$  top quark pairs and another few million single top quarks per year at low luminosity ( $10 \text{ fb}^{-1}/\text{yr}$ ). Both ATLAS [6] and CMS [7] have analyses ready for hunting out top quark FCNC processes as powerful probes for NP. With  $10 \text{ fb}^{-1}$  data, it is expected that both ATLAS and CMS could observe  $t \rightarrow q\gamma$  decays if their branching ratios are enhanced to  $\mathcal{O}(10^{-4})$  by anomalous top quark couplings [6,7]. However, if the top quark anomalous couplings are present, they will affect some precisely measured quantities with virtual top quark contributions. Inversely, these quantities can also restrict the possible number of top quark FCNC decay signals at the LHC. The precisely measured inclusive decay  $B \rightarrow X_s \gamma$  is one of the well-known sensitive probes for extensions of the SM,

especially the NP which alter the strength of FCNCs [8]. Thus, when performing the study of the possible strength of  $t \rightarrow c \gamma$  decays at the LHC, one should take into account the constraints from  $B \rightarrow X_s \gamma$  [9,10].

In this paper, we will study the contribution of anomalous  $tc\gamma$  operators to the  $\bar{B} \rightarrow X_s \gamma$  branching ratio and derive constraints on its strength. In the next section, after a brief discussion of a set of model-independent dimension 5 effective operators relevant to  $t \rightarrow c \gamma$  decay, we calculate the effects of operator  $\bar{c}_L \sigma^{\mu\nu} t_R F_{\mu\nu}$  in  $B \rightarrow X_s \gamma$  decay, which result in a modification to  $C_{7\gamma}$ . In Sec. III we present our numerical results of the constraints on its strength and the corresponding upper limits on the branching ratio of  $t \rightarrow c \gamma$  decays. Finally, conclusions are made in Sec. IV. Calculation details are presented in Appendix A, and input parameters are collected in Appendix B.

## II. TOP QUARK ANOMALOUS COUPLINGS AND THEIR EFFECTS IN $\bar{B} \rightarrow X_s \gamma$ DECAY

Without resorting to the detailed flavor structure of a specific NP model, the Lagrangian describing the top quark anomalous couplings can be written in a model-independent way with dimension 5 operators [11]

$$\begin{aligned} \mathcal{L}_5 = & -g_s \sum_{q=u,c,t} \frac{\kappa_{iqL}^g}{\Lambda} \bar{q}_R \sigma^{\mu\nu} T^a t_L G_{\mu\nu}^a \\ & - \frac{g}{\sqrt{2}} \sum_{q=d,s,b} \frac{\kappa_{iqL}^W}{\Lambda} \bar{q}_R \sigma^{\mu\nu} t_L W_{\mu\nu}^- \\ & - e \sum_{q=u,c,t} \frac{\kappa_{iqL}^\gamma}{\Lambda} \bar{q}_R \sigma^{\mu\nu} t_L F_{\mu\nu} \\ & - \frac{g}{2 \cos\theta_W} \sum_{q=u,c,t} \frac{\kappa_{iqL}^Z}{\Lambda} \bar{q}_R \sigma^{\mu\nu} t_L Z_{\mu\nu} \\ & + (R \leftrightarrow L) + \text{H.c.}, \end{aligned} \quad (1)$$

where  $\kappa$  is the complex coupling of its corresponding operator,  $\theta_W$  is the weak angle, and  $T^a$  is the Gell-Mann matrix.  $\Lambda$  is the possible new physics scale, which is unknown but may be much larger than the electroweak scale. There are also Lagrangians describing the top quark anomalous interactions with dimension 4 and 6 operators, and the dimension 4 and 5 terms can be traced back to dimension 6 operators [12,13]. In fact, top quark anomalous interactions can be generally described by the gauge-invariant effective Lagrangian with dimension 6 operators in a form without redundant operators and parameters [10,14]. A recent full list of dimension 6 operators can be found in Ref. [15]. But for on-shell gauge bosons, the Lagrangian in Eq. (1) works and is commonly employed in high energy phenomenology analysis [3,6,16].

The operators in Eq. (1) relevant to  $t \rightarrow q\gamma$  decays read

$$\begin{aligned} \mathcal{L}_\gamma = & -e \sum_{q=u,c} \frac{\kappa_{tqL}^\gamma}{\Lambda} \bar{q}_R \sigma^{\mu\nu} t_L F_{\mu\nu} \\ & - e \sum_{q=u,c} \frac{\kappa_{tqR}^\gamma}{\Lambda} \bar{q}_L \sigma^{\mu\nu} t_R F_{\mu\nu} + \text{H.c.} \end{aligned} \quad (2)$$

It is understood that the Dirac matrix  $\sigma_{\mu\nu}$  connects left-handed fields to right-handed fields. The  $t \rightarrow c\gamma$  transition will involve two independent operators  $m_q \bar{q}_R \sigma^{\mu\nu} t_L F_{\mu\nu}$  and  $m_t \bar{q}_L \sigma^{\mu\nu} t_R F_{\mu\nu}$ , where the mass factors must appear whenever a chirality flip  $L \rightarrow R$  or  $R \rightarrow L$  occurs. Because of the mass hierarchy  $m_t \gg m_c$ , the effect of  $m_q \bar{q}_R \sigma^{\mu\nu} t_L F_{\mu\nu}$  can be neglected unless  $\kappa_{tqL}^\gamma$  is enhanced to be comparable to  $\frac{m_t}{m_c} \kappa_{tqR}^\gamma$  by an unknown mechanism.

The anomalous  $tq\gamma$  coupling affects  $b \rightarrow s\gamma$  decays through the two Feynman diagrams depicted in Figs. 1(a) and 1(b). It is interesting to note that the Cabibbo-Kobayashi-Maskawa (CKM) factors in Figs. 1(a) and 1(b) are  $V_{tb}V_{qs}^*$  and  $V_{qb}V_{ts}^*$ , respectively. Since  $|V_{tb}V_{qs}^*| \gg |V_{qb}V_{ts}^*|$  for  $q = u, c$ , the contribution of Fig. 1(a) would be much stronger than that of Fig. 1(b). Furthermore, given the fact that the strengths of  $t \rightarrow u\gamma$  and  $t \rightarrow c\gamma$  are comparable, the contribution of Fig. 1(a) to  $b \rightarrow s\gamma$  is still dominated by  $t \rightarrow c\gamma$  because of  $|V_{cs}| \gg |V_{us}|$ . Hence we will only consider Fig. 1(a) with anomalous  $tc\gamma$  coupling. From the Feynman diagram of Fig. 1(a), it is easy to observe

that the large CKM factor  $V_{tb}V_{cs} \approx 1$  makes  $b \rightarrow s\gamma$  very sensitive to the strength of anomalous  $tc\gamma$  coupling.

The calculation of Fig. 1(a) can be carried out straightforwardly. The calculation details are presented in Appendix A, and the final result reads

$$\begin{aligned} i\mathcal{M}(b \rightarrow s\gamma) = & \bar{s}[e\Gamma^\nu(k)]b\epsilon_\nu(k), e\Gamma^\nu(p, k) \\ = & ie \frac{G_F}{4\sqrt{2}\pi^2} V_{cs}^* V_{tb} [i\sigma^{\nu\mu} k_\mu (m_s f_L(x) L \\ & + m_b f_R(x) R)]. \end{aligned} \quad (3)$$

Usually the  $m_s$  term can be neglected, and the function  $f_R(x)$  is calculated to be

$$\begin{aligned} f_R(x) = & \frac{\kappa_{tqR}^\gamma}{\Lambda} 2m_t \left[ -\frac{1}{(x_c - 1)(x_t - 1)} \right. \\ & - \frac{x_c^2}{(x_c - 1)^2(x_c - x_t)} \ln x_c \\ & \left. + \frac{x_t^2}{(x_t - 1)^2(x_c - x_t)} \ln x_t \right], \end{aligned} \quad (4)$$

with  $x_q = m_q^2/m_W^2$ . Now we are ready to incorporate the NP contribution into its SM counterpart for  $\bar{B} \rightarrow X_s\gamma$  decay.

In the SM, it is known that  $\bar{B} \rightarrow X_s\gamma$  decay is governed by the effective Hamiltonian at scale  $\mu = \mathcal{O}(m_b)$  [17]

$$\begin{aligned} \mathcal{H}_{\text{eff}}(b \rightarrow s\gamma) = & -\frac{4G_F}{\sqrt{2}} V_{ts}^* V_{tb} \left[ \sum_{i=1}^6 C_i(\mu) Q_i(\mu) \right. \\ & \left. + C_{7\gamma}(\mu) O_{7\gamma}(\mu) + C_{8g}(\mu) O_{8g}(\mu) \right], \end{aligned} \quad (5)$$

where  $C_i(\mu)$  are the Wilson coefficients,  $O_{i=1-6}$  are the effective four quark operators, and

$$\begin{aligned} O_{7\gamma} = & \frac{e}{16\pi^2} m_b (\bar{s}_L \sigma^{\mu\nu} b_R) F_{\mu\nu}, \\ O_{8g} = & \frac{g}{16\pi^2} m_b (\bar{s}_L \sigma^{\mu\nu} T^a b_R) G_{\mu\nu}^a. \end{aligned} \quad (6)$$

For calculating  $\mathcal{B}(\bar{B} \rightarrow X_s\gamma)$ , instead of the original Wilson coefficients  $C_i$ , it is convenient to use the so-called ‘‘effective coefficients’’ [18]

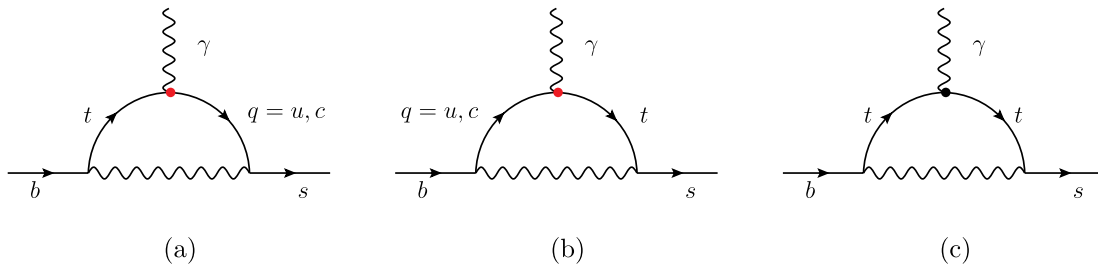


FIG. 1 (color online). Feynman diagrams for  $b \rightarrow s\gamma$ . (a) and (b) are the penguin diagrams with the anomalous  $tq\gamma$  couplings. (c) Sample LO penguin diagram in the SM.

$$C_{7\gamma}^{(0)\text{eff}}(m_b) = \eta^{16/23} C_{7\gamma}^{(0)\text{SM}}(M_W) + \frac{8}{3}(\eta^{14/23} - \eta^{16/23}) C_{8g}^{(0)\text{SM}}(M_W) + C_2^{(0)\text{SM}}(M_W) \sum_{i=1}^8 h_i \eta^{a_i}, \quad (7)$$

where  $\eta = \alpha_s(\mu_W)/\alpha_s(\mu_b)$ , and

$$h_i = \begin{pmatrix} 626/272 & 126/277 & -56/51 & 281/730 & -3/7 & -1/14 & -0.6494 \\ -0.0380 & -0.0185 & -0.0057 \end{pmatrix}, \quad (8)$$

$$a_i = \begin{pmatrix} 14/23 & 16/23 & 6/23 & -12/23 & 0.4086 & -0.4230 \\ -0.8994 & 0.1456 \end{pmatrix}. \quad (9)$$

To the leading order approximation, the  $\mathcal{B}(\bar{B} \rightarrow X_s \gamma)$  is proportional to  $|C_{7\gamma}^{(0)\text{eff}}(m_b)|^2$  [19].

In terms of the operator basis in Eq. (5), the contribution of the anomalous  $t \rightarrow c\gamma$  couplings in Eq. (3) would result in the deviation of

$$C_{7\gamma}(M_W) \rightarrow C_{7\gamma}^l(M_W) = C_{7\gamma}(M_W) + C_{7\gamma}^{\text{NP}}(M_W) \quad (10)$$

and  $C_{7\gamma}^{\text{NP}}(M_W)$  can be read from Eq. (3) as

$$C_{7\gamma}^{\text{NP}}(M_W) = \frac{\kappa_{t c R}^\gamma V_{cs}^*}{\Lambda V_{ts}^*} m_t \left[ \frac{1}{(x_c - 1)(x_t - 1)} + \frac{x_c^2}{(x_c - 1)^2(x_c - x_t)} \log x_c - \frac{x_t^2}{(x_t - 1)^2(x_c - x_t)} \ln x_t \right]. \quad (11)$$

From this equation, one can see that the NP contribution is suppressed by a factor of  $m_t/\Lambda$  but enhanced by  $V_{cs}/V_{ts}$ .

Since the NP contribution does not bring about any new operator, the renormalization group evolution of  $C_{7\gamma}^{\text{eff}}$  from  $M_W$  to the  $m_b$  scale is just the same as the SM one in Eq. (7). For  $m_t = 172$  GeV,  $m_b = 4.67$  GeV,  $\alpha_s(M_Z) = 0.118$ , and  $\Lambda = 1$  TeV, we have

$$C_{7\gamma}^{\text{eff}}(m_b) = \eta^{16/23} [C_{7\gamma}^{(0)\text{SM}}(M_W) + C_{7\gamma}^{(0)\text{NP}}(M_W)] + \frac{8}{3}(\eta^{14/23} - \eta^{16/23}) C_{8g}^{(0)\text{SM}}(M_W) + C_2^{(0)\text{SM}}(M_W) \sum_{i=1}^8 h_i \eta^{a_i} = 0.665 [C_{7\gamma}^{(0)\text{SM}}(M_W) + C_{7\gamma}^{(0)\text{NP}}(M_W)] + 0.093 C_{8g}^{(0)\text{SM}}(M_W) - 0.158 C_2^{(0)\text{SM}}(M_W) = 0.665 [-0.189 + \kappa_{t c R}^\gamma (-1.092)] + 0.093(-0.095) - 0.158. \quad (12)$$

In principle,  $C_{7\gamma}^{\text{eff}}(m_b)$  will receive corrections from anomalous  $t \rightarrow cg$  couplings in Eq. (1) which will cause a deviation to  $C_{8g}^{(0)\text{SM}}(M_W)$ . However, as shown by Eq. (12), the coefficient  $\eta^{16/23}$  of  $C_{7\gamma}^{(0)}(M_W)$  is about 1 order larger than  $\frac{8}{3}(\eta^{14/23} - \eta^{16/23})$  of  $C_{8g}^{(0)\text{NP}}(M_W)$ . Given the relative strength of  $C_{8g}^{(0)\text{NP}}(M_W)$  to  $C_{8g}^{(0)\text{SM}}(M_W)$  at 10% level,  $C_{7\gamma}^{\text{eff}}(m_b)$  will be shifted by only a few percentage. For simplifying the numerical analysis, we neglect the contribution of the anomalous  $t \rightarrow cg$  couplings. We also find that the operator  $\bar{q}_R \sigma^{\mu\nu} t_L F_{\mu\nu}$  contributes to  $\bar{B} \rightarrow X_s \gamma$  only through the term  $m_s \bar{s} \sigma_{\mu\nu} (1 - \gamma_5) b$  as shown by Eqs. (3) and (A7). Combined with the previous remarks on this operator, the effects of  $\bar{q}_R \sigma^{\mu\nu} t_L F_{\mu\nu}$  could be safely neglected.

### III. NUMERICAL RESULTS AND DISCUSSIONS

The current average of experimental results of  $\mathcal{B}(\bar{B} \rightarrow X_s \gamma)$  by the Heavy Flavor Average Group is [20]

$$\mathcal{B}^{\text{exp}}(\bar{B} \rightarrow X_s \gamma) = (3.55 \pm 0.24 \pm 0.09) \times 10^{-4}. \quad (13)$$

On the theoretical side, the next-to-leading order (NLO) calculation has been completed [19,21] and gives

$$\mathcal{B}(\bar{B} \rightarrow X_s \gamma) = (3.57 \pm 0.30) \times 10^{-4}. \quad (14)$$

The recent estimation at next-to-next-to-leading order (NNLO) [22] gives  $\mathcal{B}(\bar{B} \rightarrow X_s \gamma) = (3.15 \pm 0.23) \times 10^{-4}$ , which is about  $1\sigma$  lower than the experimental average in Eq. (13). Thus the experimental measurement of  $\mathcal{B}(\bar{B} \rightarrow X_s \gamma)$  is in good agreement with the SM predictions with roughly 10% errors on each side. The agreement would provide strong constraints on the top quark anomalous interactions beyond the SM [9,10].

The decay amplitude of  $t \rightarrow c\gamma$  has been calculated up to NLO [16]. For a consistent treatment of the constraints from  $t \rightarrow c\gamma$  and  $b \rightarrow s\gamma$  decays, we use the NLO formulas in Ref. [21] to calculate  $\mathcal{B}(\bar{B} \rightarrow X_s \gamma)$ . The experimental inputs and main formulas are collected in Appendix B. For numerical analysis, we will use the notation  $\kappa_{t c R}^\gamma = |\kappa_{t c R}^\gamma| e^{i\theta_{t c R}^\gamma}$  and set  $\Lambda = 1$  TeV.

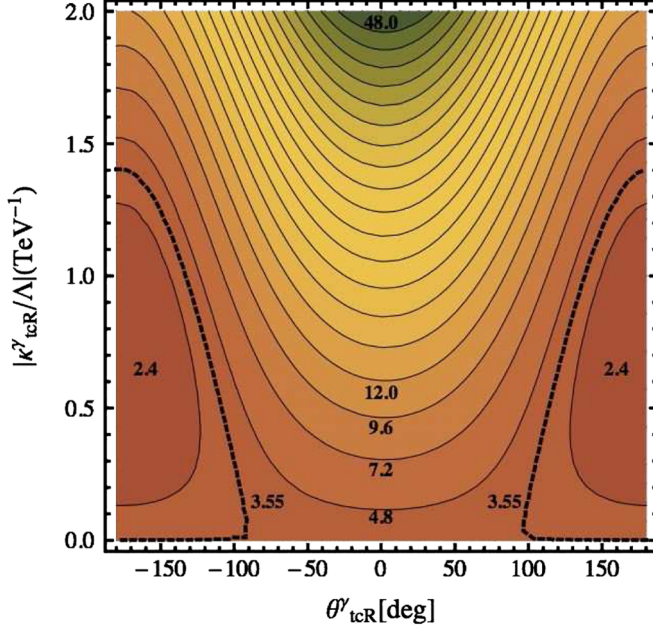


FIG. 2 (color online). The contour plot describes the dependence of  $\mathcal{B}(\bar{B} \rightarrow X_s \gamma) (\times 10^{-4})$  on  $|\kappa_{tcR}^\gamma/\Lambda|$  and  $\theta_{tcR}^\gamma$ . The dashed lines correspond to the experimental center value of  $\mathcal{B}(\bar{B} \rightarrow X_s \gamma)$ .

At first, we analyze the dependence of  $\mathcal{B}^{\text{SM}+\text{NP}}(\bar{B} \rightarrow X_s \gamma)$  on the new physics parameters  $|\kappa_{tcR}^\gamma/\Lambda|$  and  $\theta_{tcR}^\gamma$ , which is shown in Fig. 2. From the figure, one can find that the contribution of anomalous  $t \rightarrow c\gamma$  coupling is constructive to the SM one for  $\theta_{tcR}^\gamma \in [-50^\circ, 50^\circ]$ ; thus  $\mathcal{B}(\bar{B} \rightarrow X_s \gamma)$  is very sensitive to  $|\kappa_{tcR}^\gamma|$ . However, when  $|\theta_{tcR}^\gamma| \in [80^\circ, 130^\circ]$ , the sensitivity of  $\mathcal{B}(\bar{B} \rightarrow X_s \gamma)$  to  $|\kappa_{tcR}^\gamma|$  becomes weak. For  $|\theta_{tcR}^\gamma| \sim 180^\circ$ , the contribution of anomalous  $t \rightarrow c\gamma$  coupling is destructive to the SM one and there are two separated possible strengths for  $|\kappa_{tcR}^\gamma/\Lambda|$ .

The allowed region for the parameters  $|\kappa_{tcR}^\gamma/\Lambda|$  and  $\theta_{tcR}^\gamma$  under the constraints from  $\mathcal{B}(\bar{B} \rightarrow X_s \gamma)$  at 95% C.L. is shown in Fig. 3. The corresponding 95% C.L. upper bound on  $\mathcal{B}(t \rightarrow c\gamma)$  is shown in Fig. 4.

Now we discuss our numerical results. From Eq. (12), the explicit relation between the SM and the  $t \rightarrow c\gamma$  coupling contributions is

$$C_{7\gamma}^{\text{eff}}(m_b) = -0.293 - 0.726\kappa_{tcR}^\gamma. \quad (15)$$

Obviously, when  $\text{Re}\kappa_{tcR}^\gamma > 0$ , the interference between them is constructive, and it turns out to be destructive when  $\theta_{tcR}^\gamma > 90^\circ$ . Thus the features of these constraints shown in Figs. 3 and 4 for different  $\theta_{tcR}^\gamma$  are as follows:

- (i) The bound on  $|\kappa_{tcR}^\gamma/\Lambda|$  is very strong for  $\theta_{tcR}^\gamma \in [-50^\circ, 50^\circ]$ . For  $\theta_{tcR}^\gamma \approx 0^\circ$ , as shown in Fig. 3, we obtain the most restrictive upper bound  $|\kappa_{tcR}^\gamma/\Lambda| < 4.9 \times 10^{-5} \text{ GeV}^{-1}$ , which implies  $\mathcal{B}(t \rightarrow c\gamma) < 6.54 \times 10^{-5}$ .

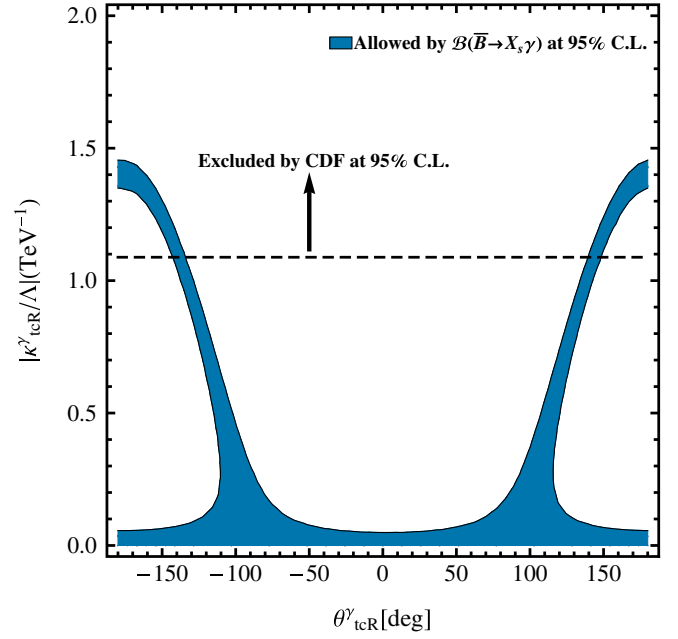


FIG. 3 (color online). The 95% C.L. upper bounds on anomalous coupling  $|\kappa_{tcR}^\gamma/\Lambda|$  as a function of  $\theta_{tcR}^\gamma$ . The shadowed region is allowed by  $\mathcal{B}^{\text{exp}}(\bar{B} \rightarrow X_s \gamma)$  and the dashed line is the CDF [5] upper limit.

- (ii) The bound on  $|\kappa_{tcR}^\gamma/\Lambda|$  is rather weak for  $\theta_{tcR}^\gamma$  around  $110^\circ$ . For such a case,  $\text{Re}\kappa_{tcR}^\gamma$  is destructive to the SM contribution as shown by Eq. (15), so, the allowed strength for the anomalous coupling is

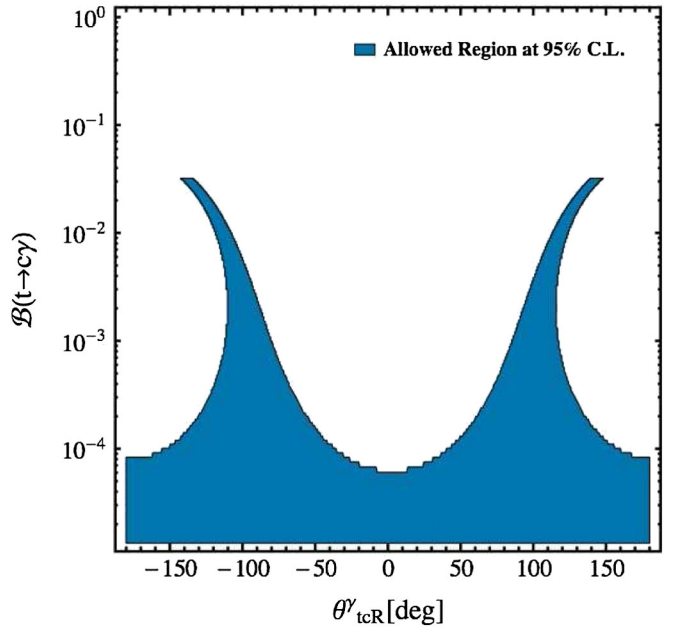


FIG. 4 (color online).  $\mathcal{B}(t \rightarrow c\gamma)$  as a function of  $\theta_{tcR}^\gamma$ . The shadowed region is allowed by the combined constraints of  $\mathcal{B}(\bar{B} \rightarrow X_s \gamma)$  and CDF searching at 95% C.L.

TABLE I. The 95% C.L. constraints on the anomalous  $t \rightarrow c\gamma$  coupling by  $\mathcal{B}(\bar{B} \rightarrow X_s \gamma)$  and  $\mathcal{B}(t \rightarrow c\gamma)$  for some specific  $\theta_{icR}^\gamma$  values.

	$\theta_{icR}^\gamma = 0^\circ$	$\theta_{icR}^\gamma = \pm 180^\circ$ S1	$\theta_{icR}^\gamma = \pm 180^\circ$ S2	$\theta_{icR}^\gamma = \pm 110^\circ$
$\mathcal{B}(\bar{B} \rightarrow X_s \gamma)$	$ \kappa_{icR}^\gamma  < 0.049$	$ \kappa_{icR}^\gamma  < 0.056$	$1.35 <  \kappa_{icR}^\gamma  < 1.45$	$ \kappa_{icR}^\gamma  < 0.55$
$\mathcal{B}(t \rightarrow c\gamma)$ CDF bounds [5]	$ \kappa_{icR}^\gamma  < 1.09$	$ \kappa_{icR}^\gamma  < 1.09$	$ \kappa_{icR}^\gamma  < 1.09$	$ \kappa_{icR}^\gamma  < 1.09$
Combined bounds	$ \kappa_{icR}^\gamma  < 0.049$	$ \kappa_{icR}^\gamma  < 0.056$	...	$ \kappa_{icR}^\gamma  < 0.55$
$\mathcal{B}(t \rightarrow c\gamma)$	$< 6.54 \times 10^{-5}$	$< 8.52 \times 10^{-5}$	...	$< 8.17 \times 10^{-3}$

much larger than the one for real  $\kappa_{icR}^\gamma$ . When  $|\theta_{icR}^\gamma| \approx 135^\circ$  and  $|\kappa_{icR}^\gamma| \approx 0.571$ ,  $C_{7\gamma}^{\text{eff}}(m_b)$  is almost imaginary since  $\text{Re}C_{7\gamma}^{\text{eff}}(m_b) \approx 0$ . Then the restriction on  $|\kappa_{icR}^\gamma/\Lambda|$  is provided by the CDF search for  $\mathcal{B}(t \rightarrow c\gamma)$  [5].

- (iii) As shown in Fig. 3, when  $\theta_{icR}^\gamma \sim \pm 180^\circ$ , there are two solutions for  $|\kappa_{icR}^\gamma/\Lambda|$ . The larger one  $|\kappa_{icR}^\gamma/\Lambda| \sim 1.4 \times 10^{-3} \text{ GeV}^{-1}$  (S2 column in Table I) corresponds to the situation in which the sign of  $C_{7\gamma}^{\text{eff}}$  is flipped. However, it has been excluded by the CDF upper bound of  $\mathcal{B}(t \rightarrow c\gamma) < 0.032$  [5]. The other solution (S1 column in Table I)  $|\kappa_{icR}^\gamma/\Lambda| < 5.6 \times 10^{-5} \text{ GeV}^{-1}$  will result in the upper limit  $\mathcal{B}(t \rightarrow c\gamma) < 8.52 \times 10^{-5}$ .

Taking  $\theta_{icR}^\gamma = 0^\circ, \pm 180^\circ$  and  $\pm 110^\circ$  as benchmarks, we summarize our numerical constraints on  $\kappa_{icR}^\gamma$  and their corresponding upper limits on  $\mathcal{B}(t \rightarrow c\gamma)$  in Table I. From the table, we can find that our indirect bound on real  $\kappa_{icR}^\gamma$  is much stronger than the CDF direct bound. The corresponding upper limits on  $\mathcal{B}(t \rightarrow c\gamma)$  are about the same order as the ATLAS sensitivity  $\mathcal{B}(t \rightarrow c\gamma) > 9.4 \times 10^{-5}$  [6] and CMS sensitivity  $\mathcal{B}(t \rightarrow c\gamma) > 4.1 \times 10^{-4}$  [7] with an integrated luminosity of  $10 \text{ fb}^{-1}$  of the LHC operating at  $\sqrt{s} = 14 \text{ TeV}$  [6].

#### IV. CONCLUSIONS

In this paper, starting with model-independent dimension 5 anomalous  $tc\gamma$  operators, we have studied their contributions to  $\mathcal{B}(\bar{B} \rightarrow X_s \gamma)$ . It is noted that the  $t \rightarrow c\gamma$  transition will involve two independent operators  $\kappa_{icR}^\gamma \bar{c}_L \sigma^{\mu\nu} t_R F_{\mu\nu}$  and  $\kappa_{icL}^\gamma \bar{c}_R \sigma^{\mu\nu} t_L F_{\mu\nu}$ . The first operator will produce a left-handed photon in  $t \rightarrow c\gamma$  decay, while the second one will produce a right-handed photon. It is found that  $\bar{B} \rightarrow X_s \gamma$  is sensitive to the first operator, but not to the second one.

For real  $\kappa_{icR}^\gamma$ , the constraint on the presence of  $\kappa_{icR}^\gamma \bar{c}_L \sigma^{\mu\nu} t_R F_{\mu\nu}$  is very strong, which corresponds to the indirect upper limits  $\mathcal{B}(t \rightarrow c\gamma) < 6.54 \times 10^{-5}$  (for positive  $\kappa_{icR}^\gamma$ ) and  $\mathcal{B}(t \rightarrow c\gamma) < 8.52 \times 10^{-5}$  (for negative  $\kappa_{icR}^\gamma$ ), respectively. These upper limits for  $\mathcal{B}(t \rightarrow c\gamma)$  are close to the  $5\sigma$  discovery sensitivities of ATLAS [6] and slightly lower than that of CMS [7] with  $10 \text{ fb}^{-1}$  integrated

luminosity operating at  $\sqrt{s} = 14 \text{ TeV}$ . For nearly imaginary  $\kappa_{icR}^\gamma$ , the constraints are rather weak since  $C_{7\gamma}$  in the SM is a real number. If  $\mathcal{B}(t \rightarrow c\gamma)$  were found to be of the order of  $\mathcal{O}(10^{-3})$  at the LHC in the future, it would imply the weak phase of  $\kappa_{icR}^\gamma$  to be around  $\pm 100^\circ$ . However, such a coupling might be ruled out by the other observable in  $B$  meson decays [23].

In summary, we have studied the interesting interplay between the precise measurement of  $b \rightarrow s\gamma$  decay at  $B$  factories and the possible  $t \rightarrow c\gamma$  decay at the LHC. For real anomalous coupling, it is shown that  $\mathcal{B}(t \rightarrow c\gamma)$  has been restricted to be below  $10^{-4}$  at 95% C.L. by  $\bar{B} \rightarrow X_s \gamma$  decay, which is already 2 orders lower than the direct upper bound from CDF [5]. The result also implies that one may need a data sample much larger than  $10 \text{ fb}^{-1}$  to hunt out  $t \rightarrow c\gamma$  signals at the LHC.

#### ACKNOWLEDGMENTS

The work is supported by the National Natural Science Foundation under Contracts No. 11075059 and No. 10735080. We thank Xinqiang Li for many helpful discussions and cross-checking calculations.

#### APPENDIX A: THE CALCULATION OF $C_{7\gamma}^{\text{NP}}(\mu_W)$

Using the Feynman rules in Fig. 5(a), the amplitude of the penguin diagram in Fig. 5(b) can be written as

$$i\mathcal{M} = \bar{u}_s(p') [e\Gamma^\nu(p, k)] u_b(p) \epsilon_\nu(k), \quad (\text{A1})$$

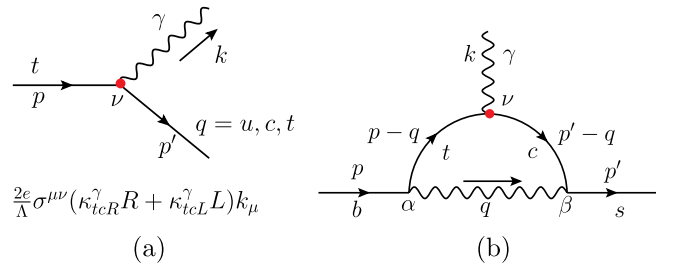


FIG. 5 (color online). (a) The Feynman rules of  $tc\gamma$  interactions in the Lagrangian of Eq. (1). (b) Penguin diagram contribution to  $b \rightarrow s\gamma$  with top quark anomalous interactions.

$$\Gamma^\nu(p, k) = -\frac{ig^2}{\Lambda} V_{cs}^* V_{tb} \int \frac{d^4 q}{(2\pi)^4} \frac{N}{[(p' - q)^2 - m_c^2 + i\epsilon][(p - q)^2 - m_t^2 + i\epsilon][q^2 - m_W^2 + i\epsilon]}, \quad (\text{A2})$$

$$N = \gamma_\alpha L(p\not{p}' - \not{q} + m_q)\sigma^{\mu\nu}(\kappa_{icR}^\gamma R + \kappa_{icL}^\gamma L) \times (\not{p} - \not{q} + m_t)\gamma_\beta L g^{\alpha\beta} k_\mu, \quad (\text{A3})$$

with  $R = (1 + \gamma^5)/2$  and  $L = (1 - \gamma^5)/2$ . By Dirac algebra

$$\gamma_\alpha L \not{q} \sigma^{\mu\nu} (\kappa_{icR}^\gamma R + \kappa_{icL}^\gamma L) \not{q} \gamma_\beta L = 0. \quad (\text{A4})$$

The terms with  $q^2$  in  $N$  vanish and  $N$  becomes

$$N = m_c \kappa_{icL}^\gamma [2(\not{p} - \not{q})\sigma^{\mu\nu} + (4 - D)\sigma^{\mu\nu}(\not{p} - \not{q})] \times L k_\mu + m_t \kappa_{icR}^\gamma [2\sigma^{\mu\nu}(\not{p}' - \not{q}) + (4 - D)(\not{p}' - \not{q})\sigma^{\mu\nu}] R k_\mu. \quad (\text{A5})$$

Thus, there is no divergence in  $\Gamma^\nu(p, k)$ . After integrating out  $q$  in the  $\Gamma^\nu(p, k)$  and using the on-shell condition,  $\Gamma^\nu(p, k)$  can be written in the following form:

$$e\Gamma^\nu(p, k) = ie \frac{G_F}{4\sqrt{2}\pi^2} V_{cs}^* V_{tb} [i\sigma^{\nu\mu} k_\mu (m_s f_L(x)L + m_b f_R(x)R)], \quad (\text{A6})$$

where

$$f_L(x) = \frac{\kappa_{icL}^\gamma}{\Lambda} 2m_c \left[ -\frac{1}{(x_c - 1)(x_t - 1)} - \frac{x_c^2}{(x_c - 1)^2(x_c - x_t)} \ln x_c + \frac{x_t^2}{(x_t - 1)^2(x_c - x_t)} \ln x_t \right], \quad (\text{A7})$$

$$f_R(x) = \frac{\kappa_{icR}^\gamma}{\Lambda} 2m_t \left[ -\frac{1}{(x_c - 1)(x_t - 1)} - \frac{x_c^2}{(x_c - 1)^2(x_c - x_t)} \ln x_c + \frac{x_t^2}{(x_t - 1)^2(x_c - x_t)} \ln x_t \right]. \quad (\text{A8})$$

Using the convention of Ref. [19], we have

$$C_{7\gamma}^{(0)\text{NP}}(M_W) = -\frac{1}{2} \frac{V_{cs}^*}{V_{ts}^*} f_R(x) = \frac{V_{cs}^*}{V_{ts}^*} m_t \frac{\kappa_{icR}^\gamma}{\Lambda} \left[ \frac{1}{(x_c - 1)(x_t - 1)} + \frac{x_c^2}{(x_c - 1)^2(x_c - x_t)} \ln x_c - \frac{x_t^2}{(x_t - 1)^2(x_c - x_t)} \ln x_t \right]. \quad (\text{A9})$$

## APPENDIX B: MAIN FORMULAS AND INPUTS

Following the notation in Ref. [21], the branching ratio of  $\bar{B} \rightarrow X_s \gamma$  can be expressed as

$$\mathcal{B}[\bar{B} \rightarrow X_s \gamma]_{E_\gamma > E_0} = \mathcal{B}^{\text{exp}}[\bar{B} \rightarrow X_c e \bar{\nu}] \left| \frac{V_{ts}^* V_{tb}}{V_{cb}} \right|^2 \frac{26\alpha_{\text{em}}}{\pi C} [P(E_0) + N(E_0)], \quad (\text{B1})$$

where  $P(E_0)$  is the perturbative ratio

$$\frac{\Gamma[\bar{B} \rightarrow X_s \gamma]_{E_\gamma > E_0}}{|V_{cb}/V_{ub}|^2 \Gamma[\bar{B} \rightarrow X_u e \bar{\nu}]} = \left| \frac{V_{ts}^* V_{tb}}{V_{cb}} \right|^2 \frac{26\alpha_{\text{em}}}{\pi} P(E_0), \quad (\text{B2})$$

which includes the Wilson coefficients of Eq. (7).  $N(E_0)$  denotes the nonperturbative corrections. The semileptonic phase space factor

$$C = \left| \frac{V_{ub}}{V_{cb}} \right|^2 \frac{2\Gamma[\bar{B} \rightarrow X_c e \bar{\nu}]}{\Gamma[\bar{B} \rightarrow X_u e \bar{\nu}]} \quad (\text{B3})$$

can be obtained from a fit of the experimental spectrum of the  $\bar{B} \rightarrow X_c l \bar{\nu}$  [24].

For calculating  $\mathcal{B}(t \rightarrow c\gamma)$ , we use the NLO formulas in Refs. [16,25]. Because  $t \rightarrow bW$  is the dominant top quark decay mode, the branching ratio of  $t \rightarrow c\gamma$  is defined as

$$\mathcal{B}(t \rightarrow c\gamma) = \frac{\Gamma(t \rightarrow c\gamma)}{\Gamma(t \rightarrow bW)}. \quad (\text{B4})$$

The partial width  $\Gamma(t \rightarrow c\gamma)$  at the NLO can be found in Ref. [16], namely,

$$\Gamma_{\text{NLO}}(t \rightarrow c\gamma) = \frac{2\alpha_s}{9\pi} \Gamma_0(t \rightarrow c\gamma) \left[ -3 \log\left(\frac{\mu^2}{m_t^2}\right) - 2\pi^2 + 8 \right], \quad (\text{B5})$$

where  $\Gamma_0(t \rightarrow c\gamma) = \alpha m_t^3 (\kappa_{icR}^\gamma / \Lambda)^2$  is the LO partial decay width.

The partial width of  $t \rightarrow bW$  has been calculated in Ref. [25] at the NLO, which reads

TABLE II. Experimental inputs for calculating the branching ratios of  $\bar{B} \rightarrow X_s \gamma$  and  $t \rightarrow c \gamma$ .

Experimental inputs	
$\alpha_{\text{em}} = 1/137.036$ [26]	$M_Z = 91.1876 \pm 0.0021$ GeV [26]
$\alpha_s(M_Z) = 0.1184 \pm 0.0007$ [26]	$M_W = 80.399 \pm 0.023$ GeV [26]
$G_F = 1.16637 \times 10^{-5}$ GeV <sup>-2</sup> [26]	$m_b^{\text{LS}} = 4.67^{+0.18}_{-0.06}$ GeV [26]
$A = 0.812^{+0.013}_{-0.027}$ [27]	$m_c(m_c) = (1.224 \pm 0.017 \pm 0.054)$ GeV [28]
$\lambda = 0.22543 \pm 0.00077$ [27]	$m_{t,\text{pole}} = 172.0 \pm 0.9 \pm 1.3$ GeV [26]
$\bar{\rho} = 0.144 \pm 0.025$ [27]	$\mathcal{B}^{\text{exp}}[\bar{B} \rightarrow X_c e \bar{\nu}] = (10.64 \pm 0.17 \pm 0.06)\%$ [29]
$\bar{\eta} = 0.342^{+0.016}_{-0.015}$ [27]	$C = 0.580 \pm 0.016$ [24]
$ V_{ts}^* V_{tb}/V_{cb} ^2 = 0.9625$	$\epsilon_{\text{ew}} = 0.0071$ [21,30]
$(V_{us}^* V_{ub})/(V_{ts}^* V_{tb}) = -0.007 + 0.018i$	$N(E_0) = 0.0036 \pm 0.0006$ [21]
$V_{cs}^*/V_{ts}^* = -24.023 - 0.432i$	$E_0 = 1.6$ GeV

$$\Gamma_{\text{NLO}}(t \rightarrow bW) = \Gamma_0(t \rightarrow bW) \left\{ 1 + \frac{2\alpha_s}{3\pi} \left[ 2 \left( \frac{(1 - \beta_W^2)(2\beta_W^2 - 1)(\beta_W^2 - 2)}{\beta_W^4(3 - 2\beta_W^2)} \right) \ln(1 - \beta_W^2) - \frac{9 - 4\beta_W^2}{3 - 2\beta_W^2} \right. \right. \\ \left. \left. \times \ln \beta_W^2 + 2\text{Li}_2(\beta_W^2) - 2\text{Li}_2(1 - \beta_W^2) - \frac{6\beta_W^4 - 3\beta_W^2 - 8}{2\beta_W^2(3 - 2\beta_W^2)} - \pi^2 \right] \right\} \quad (\text{B6})$$

with  $\Gamma_0(t \rightarrow bW) = (G_F m_t^3 / 8\sqrt{2}\pi) |V_{tb}|^2 \beta_W^4 (3 - 2\beta_W^2)$  and  $\beta_W \equiv (1 - m_W^2/m_t^2)^{1/2}$ .

The experimental inputs are collected in Table II, in which the CKM factors are derived from the Wolfenstein parameters  $A$ ,  $\lambda$ ,  $\bar{\rho}$ , and  $\bar{\eta}$ .

- 
- [1] G. Eilam, J. L. Hewett, and A. Soni, *Phys. Rev. D* **44**, 1473 (1991); **59**, 039901 (1998).
  - [2] D. Atwood, S. Bar-Shalom, G. Eilam, and A. Soni, *Phys. Rep.* **347**, 1 (2001).
  - [3] There are many papers on top quark rare decays. For a review, we refer to M. Beneke *et al.*, [arXiv:hep-ph/0003033](https://arxiv.org/abs/hep-ph/0003033), and references therein.
  - [4] S. Chekanov *et al.* (ZEUS Collaboration), *Phys. Lett. B* **559**, 153 (2003).
  - [5] F. Abe *et al.* (CDF Collaboration), *Phys. Rev. Lett.* **80**, 2525 (1998).
  - [6] J. Carvalho *et al.* (ATLAS Collaboration), *Eur. Phys. J. C* **52**, 999 (2007); F. Veloso *et al.*, Report No. CERN-THESIS-2008-106.
  - [7] L. Benucci and A. Kyriakis, *Nucl. Phys. B, Proc. Suppl.* **177–178**, 258 (2008).
  - [8] M. Antonelli *et al.*, *Phys. Rep.* **494**, 197 (2010).
  - [9] B. Grzadkowski and M. Misiak, *Phys. Rev. D* **78**, 077501 (2008).
  - [10] P.J. Fox, Z. Ligeti, M. Papucci, G. Perez, and M.D. Schwartz, *Phys. Rev. D* **78**, 054008 (2008).
  - [11] W. Hollik, J.I. Illana, S. Rigolin, C. Schappacher, and D. Stockinger, *Nucl. Phys.* **B551**, 3 (1999); **B557**, 407(E) (1999).
  - [12] W. Buchmuller and D. Wyler, *Nucl. Phys.* **B268**, 621 (1986).
  - [13] K. Hagiwara, S. Ishihara, R. Szalapski, and D. Zeppenfeld, *Phys. Rev. D* **48**, 2182 (1993); G.J. Gounaris, F.M. Renard, and C. Verzegnassi, *Phys. Rev. D* **52**, 451 (1995); G.J. Gounaris, F.M. Renard, and N.D. Vlachos, *Nucl. Phys.* **B459**, 51 (1996); K. Whisnant, J.M. Yang, B.L. Young, and X. Zhang, *Phys. Rev. D* **56**, 467 (1997); J.M. Yang and B.L. Young, *Phys. Rev. D* **56**, 5907 (1997).
  - [14] J.A. Aguilar-Saavedra, *Nucl. Phys.* **B812**, 181 (2009).
  - [15] B. Grzadkowski, M. Iskrzyński, M. Misiak, and J. Rosiek, *J. High Energy Phys.* **10** (2010) 085.
  - [16] J.J. Zhang, C.S. Li, J. Gao, H. Zhang, Z. Li, C.P. Yuan, and T.C. Yuan, *Phys. Rev. Lett.* **102**, 072001 (2009); J. Drobnak, S. Fajfer, and Jernej F. Kamenik, *Phys. Rev. Lett.* **104**, 252001 (2010).
  - [17] A.J. Buras, [arXiv:hep-ph/9806471](https://arxiv.org/abs/hep-ph/9806471); G. Buchalla, A.J. Buras, and M.E. Lautenbacher, *Rev. Mod. Phys.* **68**, 1125 (1996).
  - [18] A.J. Buras, M. Misiak, M. Münz, and S. Pokorski, *Nucl. Phys.* **424**, 374 (1994).
  - [19] A.J. Buras, A. Czarnecki, M. Misiak, and J. Urban, *Nucl. Phys.* **B631**, 219 (2002).

- [20] E. Barberio *et al.* (Heavy Flavor Averaging Group), [arXiv:0808.1297](https://arxiv.org/abs/0808.1297).
- [21] P. Gambino and M. Misiak, *Nucl. Phys.* **B611**, 338 (2001).
- [22] M. Misiak *et al.*, *Phys. Rev. Lett.* **98**, 022002 (2007).
- [23] X. Q. Li (unpublished).
- [24] C. W. Bauer, Z. Ligeti, M. Luke, A. V. Manohar, and M. Trott, *Phys. Rev. D* **70**, 094017 (2004).
- [25] C. S. Li, R. J. Oakes, and T. C. Yuan, *Phys. Rev. D* **43**, 3759 (1991).
- [26] K. Nakamura *et al.* (Particle Data Group), *J. Phys. G* **37**, 075021 (2010). The cutoff date for this update was January 15, 2010.
- [27] J. Charles *et al.* (CKMfitter Group), *Eur. Phys. J. C* **41**, 1 (2005).
- [28] A. H. Hoang and A. V. Manohar, *Phys. Lett. B* **633**, 526 (2006).
- [29] B. Aubert *et al.* (BABAR Collaboration), *Phys. Rev. D* **81**, 032003 (2010).
- [30] P. Gambino and U. Haisch, *J. High Energy Phys.* 10 (2001) 020.